

Micrometric solar-cell coating adhesion characterization by sub-picosecond laser driven shock

Jean-Paul Cuq-Lelandais^{1,2}, Cédric Broussillou³, Laurent Berthe⁴, Michel Boustie¹, Michel Jeandin³, Emilien Lescoute¹, Thibaut De Rességuier¹, Patrick Combis² and Laurent Soulard²

Summary: Shock wave propagation and the spallation within materials induced by laser shock have been investigated for roughly three decades with a few nanosecond characteristic durations. With the latest evolution in laser technologies, one can access shorter regimes in durations, going below the picosecond. This kind of irradiation provides an ultra-short shock wave and also a thin spall ejection, about a micron thick. One possible application for this regime is an adaptation of the Laser Shock Adhesion Test (LASAT) applied for micrometric coatings. which are frequently found in the industry. LASAT experiments were performed on the LULI 100TW facility on CuInSe₂ solar-cell based films to determine the debonding threshold by inducing a dynamic tension state at the interface, an important parameter for cell production and that may have an influence on the cell lifetime. Experimental post-test results on recovered samples inform about the interface rupture mechanisms. They are completed by a numerical analysis to understand the debonding processes induced by shock waves propagation and to determine the interface strengths.

Keywords: Laser driven shocks, femtosecond laser, Adhesion test, micrometric coatings and solar-cells.

Submitted to: 1st ABM-TMS International Materials Congress – Dynamic Behavior of Materials, 26 to 30 July 2010, Rio de Janeiro - Brazil

¹ PPRIMME-ENSMA - UPR CNRS 3346 (previously LCD) – 1 Av. Clément Ader, Téléport 3, 86961 Futuroscope Cedex, France

² CEA/DAM Ile de France, 91297 Arpajon, France

³ Centre des matériaux d'Evry - Mines de Paris1MINES ParisTech, Centre des Matériaux / C2P, CNRS UMR 7633, BP 87, 91003 Evry Cedex, France

⁴ PIMM Arts et Métiers ParisTech, 151 Bd de l'Hôpital, 75013 Paris, France

Introduction

Coatings technology is nowadays widely used in numerous industry fields as aeronautics or optics. The characterisation of such systems and particularly their adhesion strength is thus important. There are conventional adhesion tests such as peel, stud-pull, scratch, bulge test. These methods are commonly used for thick coatings (i.e. 100 microns or more) but they become inaccurate when the coating is too thin.

In this study, we develop an extension of the LASer Shock Adhesion Test (LASAT) process to measure the adhesion of micrometric films on a substrate [1]. The LASAT method is based on the spallation phenomenon. It consists in generating a shock wave at the face opposite to the coating with a laser pulse irradiation. The compression wave then propagates through the substrate and is reflected on the free surface. This generates a tensile load at the interface between film and substrate (See Fig. 1) which can debond the layer if the traction amplitude is strong enough.

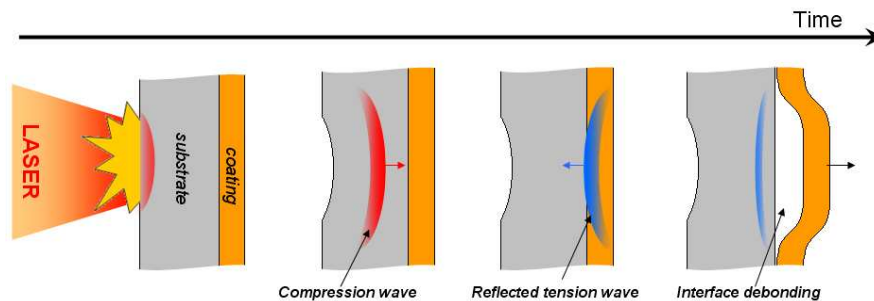


Fig. 1: Principle of LASAT (LASer Shock Adhesion Test) for measuring film-substrate interface adhesion strength

LASAT has been validated for multi-layer systems with thick substrate [2]. In this case, the adapted laser duration to debond the coating was about a few nanoseconds. In order to generate dynamic damage on a thin coating system, the characteristic shock duration, which is governed by the laser irradiation time, has to be reduced. With the improvement of sub-picosecond technologies such as the Chirped Pulse Amplification [3], it is now possible to provide increasingly short pulses, about ten femtoseconds ($1\text{fs}=10^{-15}\text{s}$) long with high intensity levels (about $1\text{PW}/\text{cm}^2=10^{15}\text{W}/\text{cm}^2$). It has recently been demonstrated it is possible to generate thin (a few microns) and reproducible spalls in aluminum targets by using a sub-picosecond laser [4, 5].

To our knowledge, this work presents the first LASAT experiments with a femtosecond laser on micrometric coated samples. The samples tested are multi-layer systems comprising a molybdenum metallic layer and a chalcopyrite CuInSe_2 semi-conductor film. Chalcopyrites $\text{Cu}(\text{In,Ga})(\text{S,Se})_2$, are considered as one of the most promising materials for thin film solar cells with record efficiencies as high as 19,9% [6]. The solar cell efficiency and stability depends on many factors and in particular the overall multilayer mechanical properties. Thus, the purpose of the experiments is to determine the interface strength between the glass substrate, the molybdenum metallic layer and the semiconductor coating.

I) Experimental setup:

The experiments were performed at the LULI's "100TW" facility¹ with a laser beam of 1.057 μm wavelength, an energy from 0.3 to 30J with a Gaussian shaped pulse having a 300fs Full Width Medium Height. The beam is concentrated on the target with a 4mm impact diameter, providing laser intensities from 10 to 100 TW/cm². Shots have been performed on multilayer targets with increasing laser intensities to detect the debonding thresholds. Because of the substrate transparency, the irradiated face of each sample has been covered with a thin aluminium layer (about 10 μm) to absorb the laser energy and generate the compression wave.

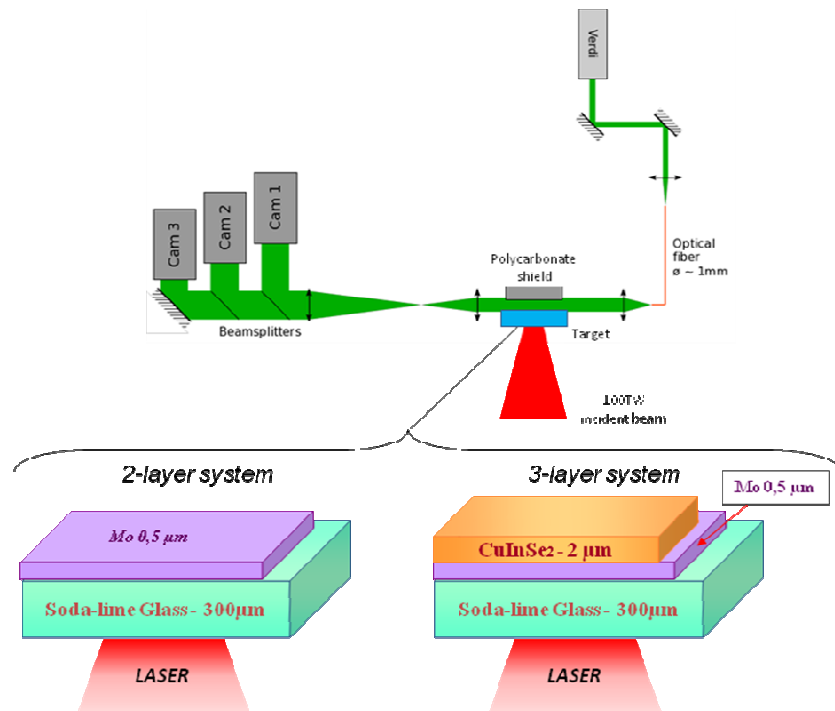


Fig.2: Schematic experimental setup and targets composition

As a diagnosis, an optical transverse shadowgraphy is used [7]. It consists in acquiring successive pictures of fragments ejected from the sample at different delay times after the laser shot. A continuous laser probe beam is injected in a 600 μm -core diameter optical fiber, and collimated with a short focus lens, to light up the gap behind the target. Imaging is done by an afocal system. The beam is divided with pelicular beamsplitters and sent to several cameras with different delay times and an acquisition duration of 50 ns, which ensures minimum motion blur (typically 5 μm for a particle ejected at 100 m/s). Quasi-instantaneous pictures of spalled layers are obtained and mean ejection velocities can be estimated.

II) Experimental results

Shots have been performed on two multilayer systems (See Fig. 2) with increasing laser intensities up to 30TW/cm². The two-layer samples have first been used to measure the Glass-Molybdenum adhesion strength by determining the loading threshold to debond the Mo coating. Then, similar procedure has been carried out for three-layer targets (the two-layer system with a CuInSe₂ layer on top) to characterize

the Mo-CuInSe₂ interface adhesion by supposing the Glass-Mo has the same behaviour as the previous shot sequence. Figure 3 sums up the experimental results, with an overview of the coated rear surface and the corresponding transverse visualization recorded during the shot. Shown samples correspond to the intensities which delimit the interfaces debonding thresholds.

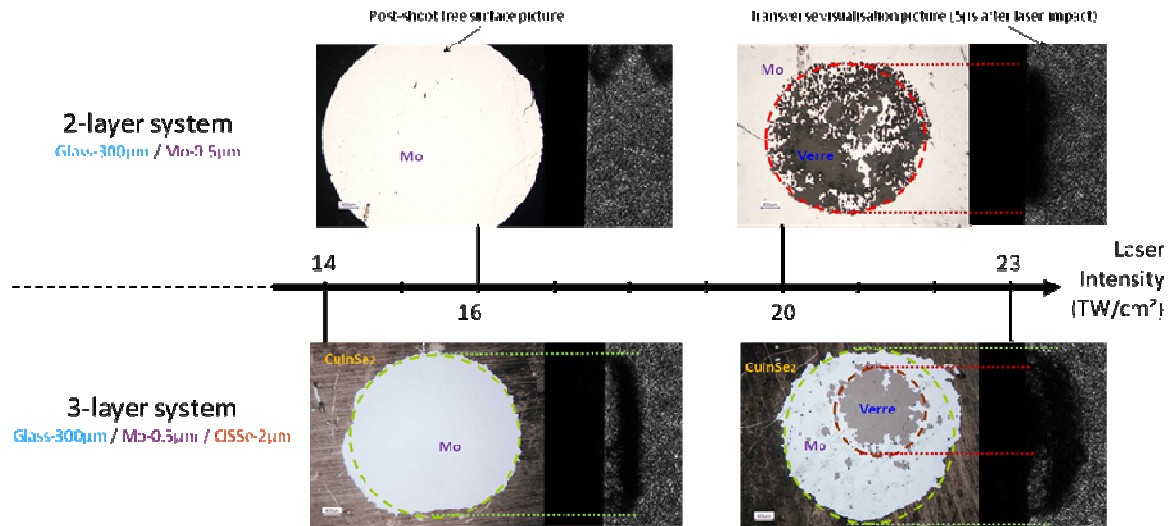


Fig.3: Overview of the free surface samples after shot (left picture for each case) and associated transverse visualizations pictures recorded 5µs after laser impact (right part of the pictures).

Concerning the 2-layer system, both the surface optical micrograph and the shadowgraphy show the Mo coating ejection for the 20TW/cm² loadcase, contrary to the lowest laser intensity shot, where no damage has been detected. In both cases, further observations evidenced no damage in the glass substrate. This confirms that the Glass-Mo adhesion threshold is delimited by: $16\text{TW/cm}^2 < \Phi_{\text{SLG-Mo}} < 20\text{TW/cm}^2$. This fact is confirmed with the 3-layer case results where the Glass-Mo interface breaks between 14 and 23 TW/cm². In this shot, one can see the two layers have been damaged, leading to a remarkable concentric circular spall figure on the free surface. The Mo layer ejection cloud can be identified on transverse visualization picture by comparison with the free surface texture. However, no shots allowed to surround the Mo-CuInSe debond intensity limit, leading to only a simple inequality: $\Phi_{\text{Mo-CuInSe}} < 14\text{TW/cm}^2$.

The mean layer front ejection velocities can be deduced from transverse visualizations and are reported in the table 1.

Sample	Intensity (TW/cm ²)	Mean ejections velocities (m/s)
Glass-Mo	16	0
Glass-Mo	20	Mo : 108 ± 15
Glass-Mo-CuInSe ₂	14	CuInSe ₂ : 171 ± 19
Glass-Mo-CuInSe ₂	23	Mo : 70 ± 8 ; CuInSe ₂ : 255 ± 18

Table 1: Average cloud particle layer velocities deduced from transverse shadowgraphy. The measured uncertainties represent the front planarity defects.

Although these values are linked to the debonding process, they do not allow to directly measure the interface strengths [2]. Only a numerical study from the laser to the layer debonding may give the necessary information to determine the stress threshold, but the experimental layer ejection velocity can be a good indicator to validate the adhesion strength deduced from simulations.

III) Numerical investigation

a) Laser-matter interaction:

Before studying the shock wave propagation in the target, it is important to characterize the mechanisms related to the laser-matter interaction in fs regime, and particularly the equivalent mechanical loading history induced. This pressure shape is determined by using the 1-D hydrodynamic laser-matter interaction code ESTHER provided by CEA-DAM [8]. This code deals with the multi-physical effects induced by an ultra-short energy deposition on condensed matter (electromagnetism, conduction, diffusion, radiative transfers...). The medium, aluminium in this study, is described by a BLF multiphase equation of state [9]. This code also includes a two temperatures model (2TM) describing the electron-ion imbalance state which influences the pressure loading shape [10].

Simulations have been performed on a few microns aluminium thick model with increasing laser intensities corresponding to those used for the experimental shots. The equivalent pressure time histories for different laser intensities Φ at a fixed depth are reported on the figure 5. The pressure profiles have a triangular shape and their FWHM duration τ_{shock} is equal to 32ps, one hundred times greater than the laser duration. Such enlargement is due to the laser-matter processes, one of them is the electron-ion equilibration, which duration is about 20ps [5].

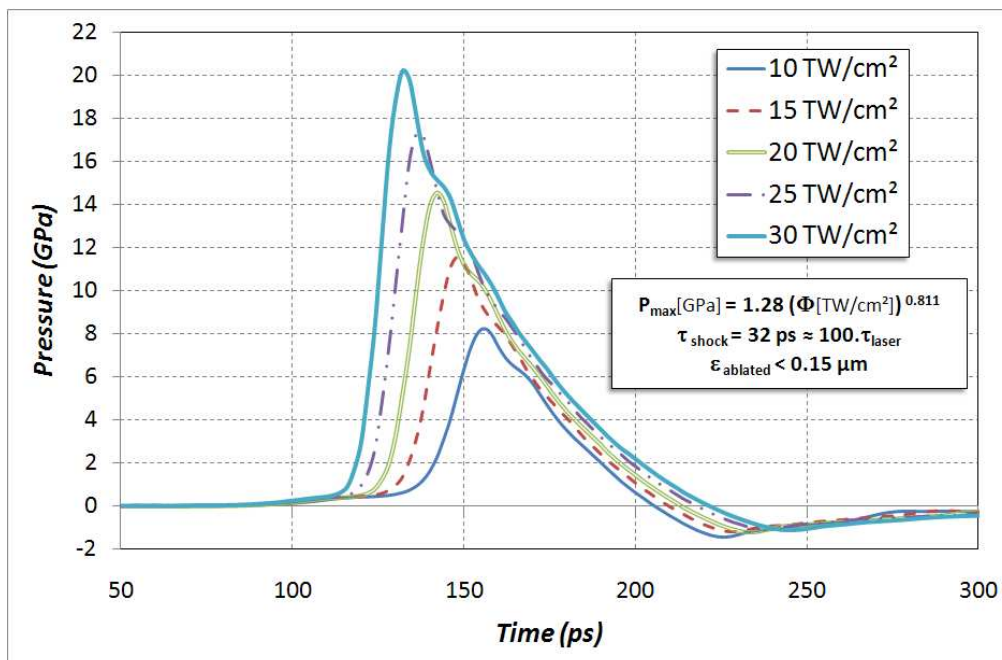


Fig.4: Equivalent pressure time histories for different laser intensities at 1 μ m depth.

The layer ablated by the laser-matter interaction is smaller than 150nm (the value corresponds to the 30TW/cm² case). However, it is experimentally observed the entire aluminium layer, a few microns thick, has been removed and there are no

evidence of phase change (droplets). This difference can be justified by the presence of a negative part in the pressure load situated behind the triangular pulse, which correspond to a traction wave. This tension state ejects the layer when traveling through the aluminium/glass interface. Thus, the negative part of the curve will not be considered next, because it is relaxed by the aluminium layer removal.

b) Shock wave propagation in the glass substrate:

Then, shock wave propagation has been modelled using the hydrocode SHYLAC from the PPRIME institute. Contrary to simple metals, the glass dynamic behaviour is still not well defined [11]. Previous studies showed singular properties as Hugoniot convexity leading to compression fans and rarefaction shocks, but also a densification process at high pressure [12]. Such material type has never been tested in an ultrafast regime as fs laser driven shock. We have thus performed simulations with a cubic interpolated Hugoniot hydrodynamic model, which is able to represent the Hugoniot convexity effects. All the parameters used in these models are listed in the table 2 [13-14].

Material	Density ρ_0 (g/cm ³)	Speed of sound c_0 (m/s)	$P_{Hugoniot}(\rho) = K_1 \cdot \eta + K_2 \eta^2 + K_3 \eta^3$; $\eta = (\rho - \rho_0) / \rho$		
			K_1 (GPa)	K_2 (GPa)	K_3 (GPa)
Soda-lime glass	2.51	5240	69.2	-234.6	331.0
Molybdenum	10.22	4910	246	361	155
CuInSe ₂	5.77	2890	48.2	96.4	84.3

Table 2: Material data for the materials used in this study [13]

We have reported on the figure 6 the pressure history at various depths of the target thickness and just before the interface.

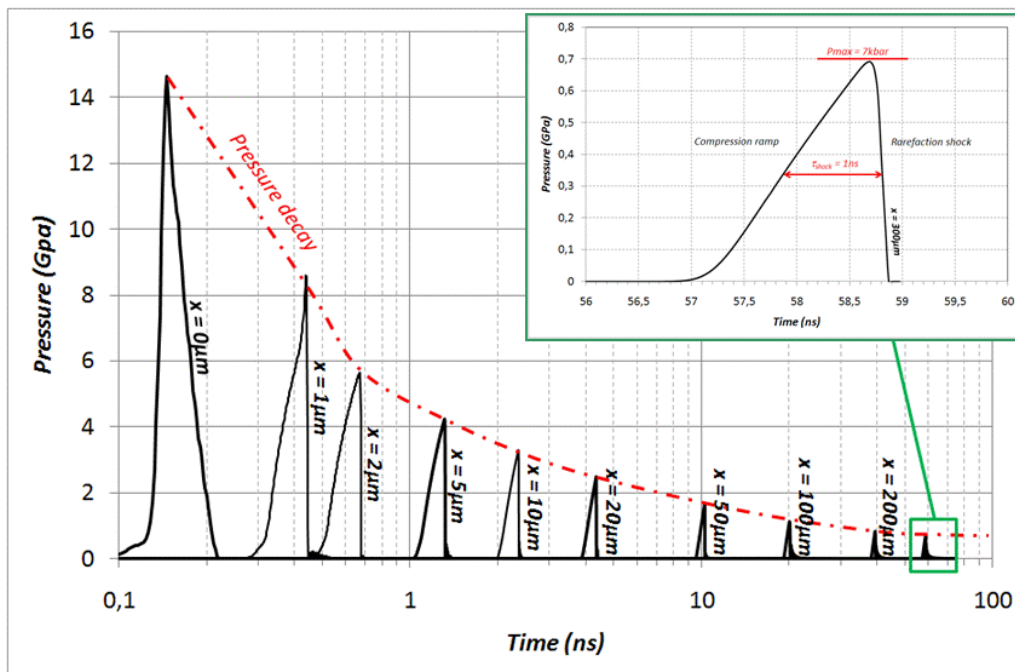


Fig.5: Pressure time histories at several fixed depth in the glass substrate for the 20TW/cm² load case.

The wave shape, initially triangular, is quickly time-reversed in the first microns by the particular glass behavior. We observe thus a compression ramp followed by a rarefaction shock. The pressure amplitude is strongly reduced and its FWHM

enlarges because of the decay which process is similar to classical shock waves. The pressure profile just before the Mo interface has a 1ns FWHM duration order and a 700MPa maximum pressure for the 20TW/cm² load case. Unfortunately, it is actually difficult to conclude if this behaviour fits with the experiments. Complementary shots should be performed with a time-resolved velocity measurement (VISAR).

c) Shock wave effects on the substrate/coating interfaces:

Even uncertainties remain concerning the glass behaviour, we showed the decay in fs regime is important and the pressure wave reaching the target rear side has become weak. We can thus suppose the glass behaviour in this zone is acoustic, which is experimentally comforted by the fact that no damage has been observed on the recovered targets. With this assumption, we analysed the shock wave propagation around the interfaces and particularly their stress history. The loading chosen is the pressure time history obtained just before the Glass-Mo interface with the densification model which appears to be the more coherent with the physical properties of soda-lime glass. The interfaces debonding have been modelled by using a cut-off damage criterion. These values are set in order to fit the experimental spall ejection velocity deduced from transverse visualisations as close as possible.

- Two-layer results:

Figure 6a and 6b present space-time diagrams for the 2-layer system zoomed in the coating vicinity. Concerning the 16TW/cm² loadcase, the incident wave propagates through the interface, inducing a reflection/transmission process. The transmitted wave is then reflected by the free surface into a tension wave, which goes back to the interface. The interface stress history (See Fig. 6a) shows the maximum value reached is 510MPa, which implies the Glass-Mo debonding threshold $\sigma_{\text{Glass-Mo}}$ is higher. Because there is no rupture in this simulation, the waves continue to travel and diffuse by multi-reflection/transmission on the interface. Contrary to the previous modelling, there is an interface breaking for 20TW/cm² experimental shot. A simulation without rupture criterion indicates a maximum interface stress equal to 620MPa. A parametric study is then performed by varying the interface cut-off threshold $\sigma_{\text{Glass-Mo}}$ between 510 and 620MPa. The aim here is to fit the average ejected layer velocity V_{Mo} with the corresponding experimental data. A good concordance is obtained for $\sigma_{\text{Glass-Mo}}=550\text{MPa}$. This value is very close from existing data (576 MPa in [15]). Figure 6.b shows the target behaviour for the 20TW/cm² numerical model. The shock wave reflection leads to the interface rupture and relaxation waves. All the waves trapped in the Mo layer contribute to eject it with a 95m/s velocity, which is close to the experimental value.

- Three-layer results:

The same approach has been applied to the complete 3-layer system. We set here the Glass-Mo strength as a constant (550MPa) and we try to determine the Mo-CuInSe₂ interface threshold $\sigma_{\text{Mo-CIS}}$. Two issues are rising for this configuration: first, experimentally no shots allowed to delimit the threshold; and then, the coated CuInSe₂ high pressure dynamic behaviour is not known with accuracy. The first results for the 23 TW/cm² without damage evidence clearly a too small maximum free surface velocity (about 85m/s), which implies the modelled ejection velocity would not overtake this value. This difference may be explained by free surface roughness

effects leading to particle microjetting [17]. This phenomenon depends on the material and the applied pressure and provides particle velocities higher than classical shock theory. Figure 7 shows an example of space-time diagram for the three layer system. In addition, a cut-off rupture criterion has been associated to the CuInSe_2 layer to observe qualitatively the fragmentation process which could lead to the experimental particle cloud ejected with a velocity on the transverse visualization.

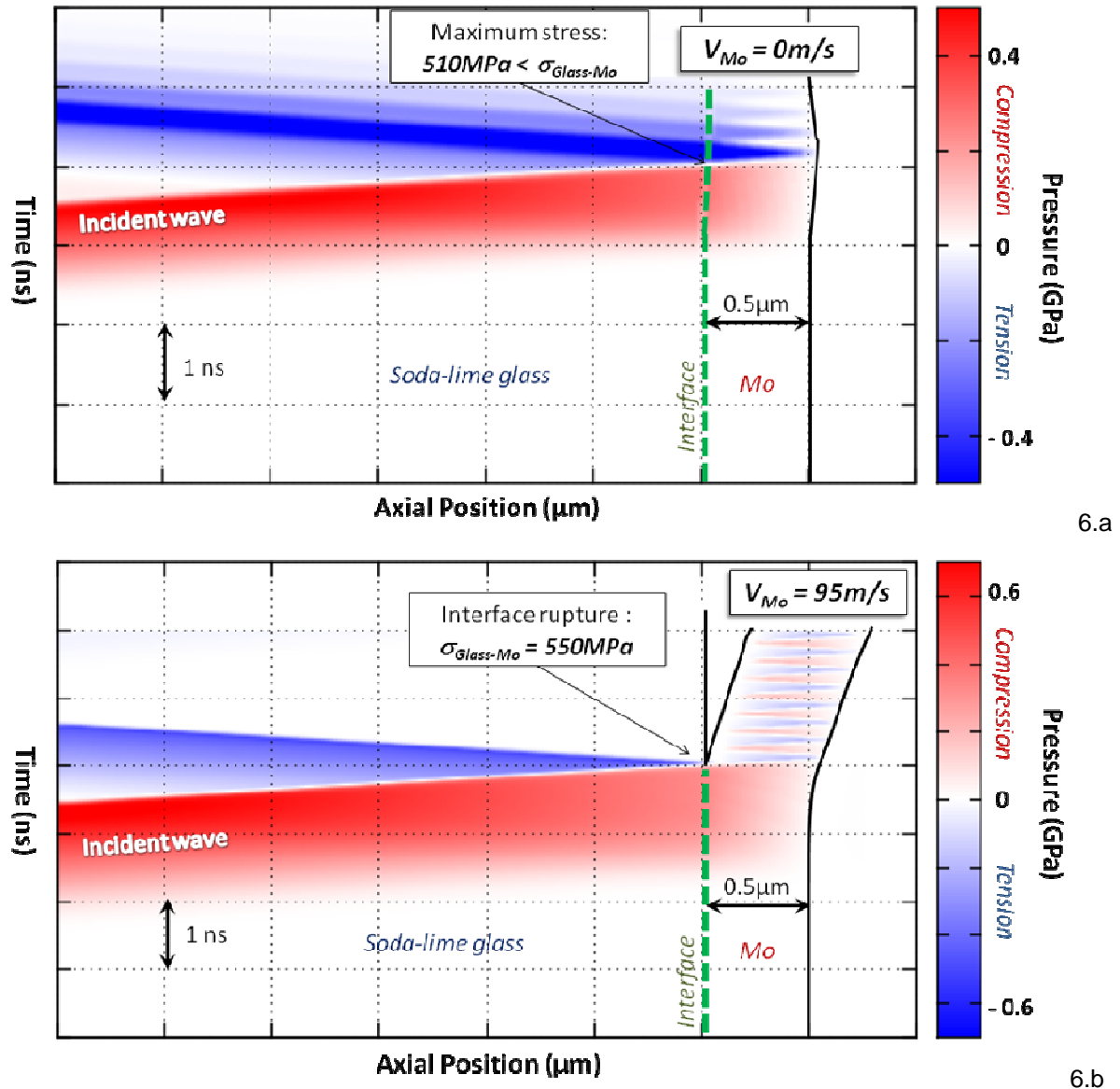


Fig.6: Space-time diagrams for the 2-layer system corresponding to the experimental shots delimiting the debonding threshold (6.a = $16\text{TW}/\text{cm}^2$ and 6.b = $20\text{TW}/\text{cm}^2$)

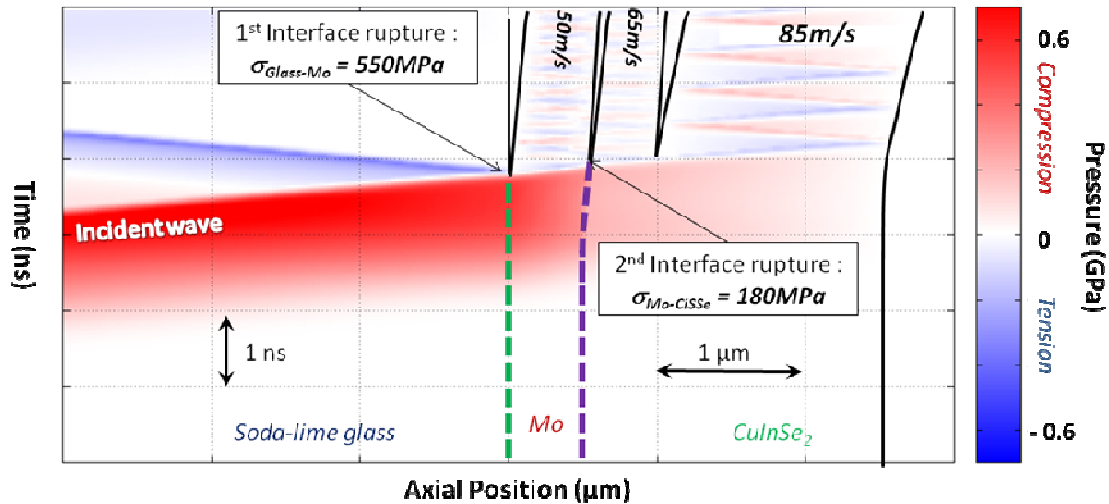


Fig.7: 3-layer target space-time diagram corresponding to the 23TW/cm² loadcase

Conclusion and future work

These experiments performed with a femtosecond laser on solar-cell based targets for the first time showed the feasibility to adapt the LASAT process to micrometric coatings. With this configuration, it is possible to eject a layer without damaging the substrate, and eventually to debond more than one coating with one shot. Shots with increasing laser intensities enabled us to estimate the Glass-Mo adhesion strength. One-dimensional simulations performed on the 2-layer system are physically coherent with shock physics and experimental ejected layer velocities. Moreover, the numerical results give access to a quantitative estimation of the adhesion strength. Additional experiments are planned to confirm the results repeatability and delimit the Mo-CuInSe₂ interface strength which is still uncertain at this time.

One other orientation for this study is to investigate the two-dimensional aspect of the configuration, and particularly the edge effects influence. This phenomenon caused by loading limited area, acts like a lateral decay which alters the radial space stress repartition [17-18]. As an example, they can be observed on these experiments through the double concentric spalled layers. The understanding and numerical prediction of the debonded area could give additional information about the interface rupture thresholds.

References

- [1] M. Arrigoni, S. Barradas, M. Braccini, M. Dupeux, M. Jeandin, M. Boustie, C. Bolis and L. Berthe, *J. Adhesion Sci. Technol.* **20(5)** 471-487 (2006)
- [2] C. Bolis, L. Berthe, M. Boustie, M. Arrigoni, S. Barradas and M. Jeandin, *Journal of Physics D: Applied Physics* **40** 3155-3163 (2007)
- [3] D. Strickland, G. Mourou, *Opt. Commun.* **56** 219 (1985)
- [4] H. Tamura, T. Kohama, K. Kondo and M. Yoshida, *J. Appl. Phys.* **89(6)** 3520-3522 (2001)
- [5] J.P. Cuq-Lelandais, M. Boustie, L. Berthe, T. De Resseguier, P. Combis, J.P. Colombier, M. Nivard and A. Claverie, *J. Phys D: Appl. Phys.* **42** 065402-065412 (2008)

- [6] I. Repins, M.A. Contreras, B. Egaas, C. DeHart, J. Scharf, C. L. Perkins, B. To and R. Noufi, *Progress in Photovoltaics* **16**, 235-239 (2008)
- [7] E. Lescoute, T. De Resseguier, J.-M. Chevalier, M. Boustie, L. Berthe and J.-P. Cuq-Lelandais, *16th APS SCCM, Nashville (TN) – USA*, 1043-1046 (2009)
- [8] J.-P. Colombier, P. Combis, R. Stoian and E. Audouard, *Phys. Rev. B* **75** 104105 (2007)
- [9] A.V. Bushman, I.V. Lomonosov and V.E Fortov, *Sov. Tech. Rev. B: Therm. Phys.* **E 47** 3547 (1993).
- [10] B. Rethfield, A. Kaiser, M. Vikanek and G. Simons, *Phys Rev B* **65** 21403 (2002)
- [11] T de Rességuier and F. Cottet, *J. Appl. Phys.* **77(8)** 3756-3761 (1995)
- [12] Z. Rozenberg, Y. Ashuach and E. Dekel, *Int. J. Imp. Engin.* **35(8)** 820-828 (2008)
- [13] "LASL Shock Hugoniot Data", Editions S.P. Marsh, University of California Press (1980).
- [14] H. Neumann, *Solar Cells* **16** 399-418 (1986)
- [15] V. Gupta, V. Kireev, J. Tian, H. Yoshida and H. Akahoshi, *Journal of the Mechanics and Physics of Solids* **51** 1395-1412 (2003)
- [16] E. Lescoute, T. De Resseguier, J.-M. Chevalier, M. Boustie, L. Berthe and J.-P. Cuq-Lelandais, *9th DYMAT, Brussels – Belgium*, 163-169 (2009)
- [17] M. Boustie, J.-P. Cuq-Lelandais, L. Berthe, C. Bolis, S. Barradas, M. Arrigoni, T. de Resseguier and M. Jeandin, *15th APS SCCM, Waikoloa, Hawaii – USA*, 1323-1326.
- [18] J.-P. Cuq-Lelandais, M. Boustie, L. Berthe, P. Combis, A. Sollier, T. De Resseguier, E. Lescoute, E. Gay, L. Soulard and J. Bontaz-Carion, *9th DYMAT, Brussels – Belgium*, 625-631 (2009)